0026-895X/11/7903-453–460$20.00
MOLECULAR PHARMACOLOGY
Vol. 79, No. 3
69708/3671600
*Mol Pharmacol* 79:453–460, 2011
*Printed in U.S.A.*




# Identification and Mechanism of Action of the Acylguanidine MRT-83, a Novel Potent Smoothened Antagonist[S]

Hermine Roudaut, Elisabeth Traiffort, Tatiana Gorojankina, Ludwig Vincent, Helene Faure, Angele Schoenfelder, Andre Mann, Fabrizio Manetti, Antonio Solinas, Maurizio Taddei, and Martial Ruat

*Signal Transduction and Developmental Neuropharmacology Team, Institut de Neurobiologie Alfred Fessard IFR2118, Laboratoire de Neurobiologie et Développement, Centre National de la Recherche Scientifique, UPR-3294, Gif-sur-Yvette, France (H.R., E.T., T.G., L.V., H.F., M.R.); Laboratoire d'Innovation Thérapeutique, Centre National de la Recherche Scientifique, Unité Mixte de Recherche-7200, Université de Strasbourg, Illkirch, France (A.S., A.M.); and Dipartimento Farmaco Chimico Tecnologico, Università degli Studi di Siena, Siena, Italy (F.M., A.S., M.T.)*

Received October 29, 2010; accepted December 21, 2010

## ABSTRACT

There is a clear need to develop novel pharmacological tools to improve our understanding of Smoothened (Smo) function in normal and pathological states. Here, we report the discovery, the mechanism of action, and the in vivo activity of *N*-(2-methyl-5-(3-(3,4,5-trimethoxybenzoyl)guanidino)phenyl)biphenyl-4-carboxamide (MRT-83), a novel potent antagonist of Smo that belongs to the acylguanidine family of molecules. MRT-83 fits to a proposed pharmacophoric model for Smo antagonists with three hydrogen bond acceptor groups and three hydrophobic regions. MRT-83 blocks Hedgehog (Hh) signaling in various assays with an $IC_{50}$ in the nanomolar range, showing greater potency than the reference Smo antagonist cyclopamine. MRT-83 inhibits Bodipy-cyclopamine binding to human and mouse Smo but does not modify Wnt signaling in human embryonic kidney 293 transiently transfected with a Tcf/Lef-dependent Firefly luciferase reporter together with a *Renilla reniformis* luciferase control reporter. MRT-83 abrogates the agonist-induced trafficking of endogenous mouse or human Smo to the primary cilium of C3H10T1/2 or NT2 cells that derive from a pluripotent testicular carcinoma. Stereotaxic injection into the lateral ventricle of adult mice of MRT-83 but not of a structurally related compound inactive at Smo abolished up-regulation of *Patched* transcription induced by Sonic Hedgehog in the neighboring subventricular zone. These data demonstrate that MRT-83 efficiently antagonizes Hh signaling in vivo. All together, these molecular, functional and biochemical studies provide evidence that MRT-83 interacts with Smo. Thus, this novel Smo antagonist will be useful for manipulating Hh signaling and may help develop new therapies against Hh-pathway related diseases.

## Introduction

The Hedgehog (Hh) signaling pathway is implicated in developmental processes and in multiple physiological responses in adult tissues, including the control of brain functions. Hh pathway activation in vertebrates requires binding of a Hh peptide to the 12-pass transmembrane protein Patched (Ptc), which, in the absence of its ligand, represses the activation of the seven-pass transmembrane protein Smoothened (Smo), a proposed member of the G-protein-coupled receptor (GPCR) family. Upon Smo activation, a complex signaling cascade is initiated, leading to activation of Gli transcription factors and gene transcription (Beachy et al., 2004; Dessaud et al., 2008; Traiffort et al., 2010). Thus, most Smo-associated responses have been linked to tran-

This work was supported by a grant from La Ligue Contre le Cancer (Comité des Yvelines); and the Neuropole de Recherche Francilien [doctoral fellowship 248890] (to H.R.).
Article, publication date, and citation information can be found at http://molpharm.aspetjournals.org.
doi:10.1124/mol.110.069708.
[S] The online version of this article (available at http://molpharm.aspetjournals.org) contains supplemental material.

**ABBREVIATIONS:** Hh, Hedgehog; Ptc, Patched; Smo, Smoothened; GPCR, G-protein-coupled receptor; BCC, basal cell carcinoma; MRT-83, *N*-(2-methyl-5-(3-(3,4,5-trimethoxybenzoyl)guanidino)phenyl)biphenyl-4-carboxamide; Cur61414, *N*-((3*S*,5*S*)-1-(benzo[*d*][1,3]dioxol-5-ylmethyl)-5-(piperazine-1-carbonyl)pyrrolidin-3-yl)-*N*-(3-methoxybenzyl)-3,3-dimethylbutanamide; MRT-36, 3,4-dimethoxy-*N*-(phenylcarbamothioyl)benzamide; SVZ, subventricular zone; BC, Bodipy-cyclopamine; IWR1, 4-(1,3,3*a*,4,7,7*a*-hexahydro-1,3-dioxo-4,7-methano-2*H*-isoindol-2-yl)-*N*-8-quinolinyl-benzamide; SAG, Smoothened agonist; Shh, Sonic hedgehog; ShhN, Sonic hedgehog N terminus; DMSO, dimethyl sulfoxide; HEK, human embryonic kidney; FCS, fetal calf serum; DAPI, 4,6-diamidino-2-phenylindole; GCP, granule cell precursor; MS, medial septum; LV, lateral ventricle; ISH, in situ hybridization.

scriptional activities mediated by Hh signaling. However, recent data suggest that some physiological responses do not involve gene transcription and are observed upon short activation of Smo (Yam et al., 2009; Traiffort et al., 2010). Trafficking of Hh signaling components at the primary cilium is proposed to regulate Hh pathway activities. In the absence of its ligand, Ptc is localized at the primary cilium as evidenced in neural tube cells during development (Rohatgi et al., 2007). Upon Hh binding, Ptc traffics out of the cilium and Smo translocates into it (Corbit et al., 2005). The biochemical and molecular mechanisms regulating Smo trafficking are complex and presumably involve multiple states of Smo that might be modulated by Ptc itself. Small molecules acting at Smo have been shown to modify Smo trafficking at the primary cilium, and the mechanism of antagonist action to block Smo translocation at the primary cilium has been proposed to be relevant in cancer therapies (Rohatgi et al., 2009; Wang et al., 2009; Wilson et al., 2009).

During the last decade, autocrine and paracrine Hh signaling have been linked to cancers, and molecules aimed at inhibiting the pathway have been proposed to be of interest for alleviating the associated symptoms (Scales and de Sauvage, 2009). The Hh pathway is activated by oncogenic Ptc and Smo mutations observed in basal cell carcinoma (BCC) or medulloblastoma. Such Hh pathway activation, which is ligand-independent, is also observed in Gorlin syndrome, in which patients present Ptc-inactivating mutations that render them highly susceptible to the development of BCC, medulloblastoma, and rhabdomyosarcoma (Barakat et al., 2010). Characterization of Hh component trafficking to the primary cilium is of interest for further clarifying the role of Hh signaling in various types of cancers.

Cyclopamine, a natural and teratogenic compound, and several other small-molecule Hh pathway inhibitors have been developed and proposed for the treatment of cancers associated with dysfunctions of Hh signaling. Most of these molecules, but not all, target Smo (Scales and de Sauvage, 2009; Peukert and Miller-Moslin, 2010). The initial trials for treating BCC using cyclopamine in humans have not been followed up. However, cyclopamine derivatives have been developed and are under investigation for the treatment of various Hh-linked cancers. Other Smo antagonists, such as *N*-((3*S*,5*S*)-1-(benzo[*d*][1,3]dioxol-5-ylmethyl)-5-(piperazine-1-carbonyl)pyrrolidin-3-yl)-*N*-(3-methoxybenzyl)-3,3-dimethylbutanamide (Cur61414) or HhAntag691 have been shown to induce remission in animal models of medulloblastoma or BCC (Scales and de Sauvage, 2009). Clinical trials for treating BCC and medulloblastoma in humans have been conducted with the small molecule GDC-0449 (vismodegib), which displays nanomolar potency for inhibiting Smo. However, such molecules may have some limitations associated with Smo mutations leading to treatment resistance, as reported recently in one case of medulloblastoma (Rudin et al., 2009; Von Hoff et al., 2009; Yauch et al., 2009). Still, Smo inhibitors may have other clinical applications, such as the treatment of unwanted hair related to their inhibiting activity on hair growth (Li et al., 2010). Pharmacological inhibition of Hh signaling using a Smo antagonist has also been shown to reduce the severity of osteoarthritis in mice models suggesting a therapeutic approach to cartilage degeneration (Lin et al., 2009).

Herein, we report our efforts to identify and characterize novel small molecules inhibiting Smo with high potency. We have synthesized *N*-(2-methyl-5-(3-(3,4,5-trimethoxybenzoyl) guanidino)phenyl)biphenyl-4-carboxamide (MRT-83), a novel acylguanidine derivative that shows nanomolar antagonist potency toward Smo in various Hh assays. MRT-83 also blocks Hh-mediated Ptc transcription in the subventricular zone (SVZ) of adult mice in vivo indicating that this inhibitor should be useful for investigating Hh pathway-dependent responses in both normal and pathological conditions.

## Materials and Methods

**Drugs.** Cyclopamine and Bodipy-cyclopamine (BC) were from Toronto Research Chemicals Inc. (North York, ON, Canada). 3,4-Dimethoxy-*N*-(phenylcarbamothioyl)benzamide (MRT-36) was from ASINEX (Rijswijk, The Netherlands). 4-(1,3,3*a*,4,7,7*a*-Hexahydro-1,3-dioxo-4,7-methano-2*H*-isoindol-2-yl)-*N*-8-quinolinyl-benzamide (IWR1; Chen et al., 2009) was from Sigma (Saint-Quentin Fallavier, France). SAG was synthesized as described previously (Martínez et al., 2006). Details of the synthesis and structural characterization of MRT-83 are available upon request. ShhN was from R&D Systems (C24II) for [$^3$H]thymidine incorporation or was provided by Dr. D. Baker (Biogen Idec, Boston, MA) for the other experiments. SAG and cyclopamine were dissolved in ethanol, and other compounds were dissolved in DMSO at a concentration of 10 mM. [$^3$H]Thymidine was from PerkinElmer Life and Analytical Sciences (Courtaboeuf, France).

**Pharmacophoric Model of MRT-83.** We constructed a pharmacophoric model of MRT-83 based on chemical structures of Smo inhibitors as described previously (Manetti et al., 2010).

**Plasmids.** The plasmids pRK5 and pRK5-SP-myc-Smo encoding the mouse Smo sequence have been described previously (Manetti et al., 2010) and are referred to in the text as pRK5 and mouse Smo, respectively. The Wnt reporter plasmid M50 Super8xTOPFlash containing seven Tcf/Lef binding sites in the firefly luciferase promoter, the pLNCWnt-3aHA, and the control pRL-TK *Renilla reniformis* luciferase were obtained from Addgene (Cambridge, MA).

**Antibodies.** A previously described polyclonal rabbit antiserum against rat Smo was used (Masdeu et al., 2007). The mouse anti-acetylated tubulin antibody and the mouse monoclonal anti-c-myc antibody were obtained from Sigma; the goat anti-mouse Alexa Fluor 546 antibody was obtained from Invitrogen (Leiden, The Nederlands); and the goat anti-rabbit fluorescein isothiocyanate antibody from Millipore Bioscience Research Reagents (Temecula, CA).

**Cell Culture and Transfection.** Zeocin, Geneticin (G418), penicillin-streptomycin, and all cell culture media or products were from Invitrogen (Cergy Pontoise, France) except as stated otherwise. HEK293 (American Type Culture Collection, Manassas, VA) and C3H10T1/2 (American Type Culture Collection) were cultured in Dulbecco's modified Eagle's medium supplemented with 10% fetal calf serum (FCS) as described previously (Manetti et al., 2010). The Shh-light2 cells (from Pr. P. A. Beachy, Stanford University, Stanford, CA) and HEK-hSmo cells stably expressing human Smo were cultured in the same medium supplemented with 0.4 mg/ml G418 and 0.150 mg/ml Zeocin or 0.5 mg/ml G418, respectively. NT2 cells (American Type Culture Collection) were cultured in Opti-MEM (Invitrogen) supplemented with 10% FCS. HEK293 cells were transiently transfected by electroporation using 4 $\mu$g of mouse Smo and 6 $\mu$g of pRK5 for BC binding. For Tcf/Lef-dependent luciferase reporter assay, HEK293 were transfected by FuGENE (Roche Diagnostics, Mannheim, Germany) with 0.1 $\mu$g of Tcf/Lef reporter, 0.25 $\mu$g of *R. reniformis* luciferase and, as indicated in the legend to Fig. 3, with 0.1 $\mu$g of Wnt3a plasmids, supplemented to 0.4 $\mu$g/well with pRK5 plasmid. Cells were distributed into six-well plates containing glass coverslips coated with 0.05 mg/ml poly-D-lysine (BD Biosciences, Le Pont de Claix, France) for BC binding, Smo ciliary accumulation, and immunofluorescence experiments, or alternatively

into 96- or 24-well plates for [$^3$H]thymidine analysis and Tcf/Lef-dependent luciferase reporter assay.

**Stable Expression of Human Smo in HEK293 Cells.** To generate the myc-human Smo construct, the human Smo sequence encoding the full-length protein devoid of the first 31 amino acids was amplified by polymerase chain reaction from the pCR2.1-hSmo vector kindly provided by Dr I. Mus-Veteau (University Nice-Sophia Antipolis, France), subcloned into pRK5-SP-myc vector (Manetti et al., 2010), using the restriction sites MluI and SalI to give pRK5-SP-myc-hSmo plasmid. The nucleotide sequence of hSmo construct was verified by DNA sequencing. HEK293 cells were transfected using FuGENE with pRK5-SP-myc-hSmo together with the expression vector pcDNA3 (Invitrogen) containing the selection marker neomycin. Transfected cells were selected with 2 mg/ml G418 and one clone (HEK-hSmo) selected for its expression of Smo by immunofluorescence using anti-c-myc antibodies was further characterized.

**Gli-Dependent Luciferase Reporter Assay.** Shh-light2 cells were incubated for 40 h with ShhN (5 nM) and the studied compounds. The cell-based bioassay was performed as described previously (Manetti et al., 2010).

**Tcf/Lef Dependent Luciferase Reporter Assay.** After transfection (1 h) with the Wnt reporter and the control *R. reniformis* luciferase plasmids, HEK293 cells were incubated with MRT-83 (5 $\mu$M), IWR1 (10 $\mu$M), or vehicle (DMSO) alone, and luciferase activities were measured 48 h later. Data are Firefly luciferase activity reported relative to the *R. reniformis* luciferase control activity. The MRT-83 compound did not significantly modify the *R. reniformis* luciferase activity at 5 $\mu$M.

**Alkaline Phosphatase Assay.** C3H10T1/2 cells were incubated for 6 days in the presence of SAG (0.1 $\mu$M) and the studied compounds. The cell-based bioassay was performed as described previously (Manetti et al., 2010).

**BC Binding.** The protocol was adapted from (Manetti et al., 2010). BC (green) and DAPI (blue; Vector Laboratories, Burlingame, CA) signals were analyzed in three to four representative fields per coverslip (~800 cells/field). The fluorescence intensity of transfected cells determined in presence of BC (5 nM) alone or in the presence of the drugs, over the basal fluorescence measured in the absence of BC was quantified and divided by the area occupied by the nuclei (DAPI staining) in the field. Data were expressed as percentage of fluorescence intensity observed with BC alone.

**Primary Cerebellar Cultures.** Isolation of cerebellar granule cell precursors (GCPs) and quantitation of [$^3$H]thymidine incorporation were performed as described previously (Charytoniuk et al., 2002a).

**Ciliary Smo Accumulation Assay.** The protocol was adapted from that of Rohatgi et al. (2009). After 24 h of culture, C3H10T1/2 or NT2 cells were switched to Dulbecco's modified Eagle's medium or Opti-MEM, respectively, containing 0.5% FCS in the presence of SAG, MRT-83, cyclopamine, or vehicle solutions for 18 h. Then, cells were fixed with paraformaldehyde (4%) in PBS for 20 min, washed, incubated with a 0.05% Triton X-100 PBS solution for 5 min, and washed in a blocking gelatin-PBS (0.2%) solution. Primary antibodies (1:2000 for anti-Smo, 1:5000 for anti-acetylated tubulin) were diluted in the blocking solution supplemented with 1% normal goat serum. Cells were incubated for 2 h at room temperature. After washes in gelatin-PBS, secondary antibodies were added (1:1000) in fresh blocking solution for 90 min at room temperature. Cells were finally washed in gelatin-PBS solution and mounted in Vectashield DAPI. Acetylated tubulin (red) and Smo (green) were analyzed in three or four representative fields by coverslip (100 cells/field). In each field, the percentage of cells expressing cilium remained stable. The percentage of ciliary Smo reflects the number of cells that display a Smo/acetylated tubulin colocalization.

**Data Analysis.** Means and S.E.M. were calculated using Excel 2003 (Microsoft Corp, Redmond, WA). Curve fitting and $IC_{50}$ determinations were performed using Prism 4.03 (GraphPad Software, San Diego, CA). The BC fluorescence was analyzed with the Simple-PCI software (Hamamatsu Corporation, Massy, France).

**Animals and Treatment.** The protocol of injection has been done according to a procedure described previously (Angot et al., 2008). Four groups of six animals received 5 $\mu$l of 45% 2-hydroxypropyl-$\beta$-cyclodextrin (Sigma) PBS solution containing 0.9 $\mu$g of ShhN alone or in the presence of MRT-83 (200 ng) or MRT-36 (110 ng). A control group received 5 $\mu$l of 45% 2-hydroxypropyl-$\beta$-cyclodextrin solution alone. All groups were analyzed 48 h after the injection. All procedures were carried out in accordance with the European Community Council Directive (86/806/EEC) for the care and use of laboratory animals.

**In Situ Hybridization.** The experiments using Ptc-specific riboprobes were performed as described previously (Angot et al., 2008).

**Counting and Statistical Analysis.** The number of Ptc-positive cells was counted between bregma levels +0.18 and +0.38 mm along the SVZ or in a representative field of the medial septum (MS) on each section. Analysis was carried out on at least three sections per animal. Statistical analysis was performed using the Student's $t$ test. Statistical significance was considered for $p < 0.05$.

**Microscopy.** Both cell cultures and tissue slices were analyzed with a DMRXA2 microscope (Leica Microsystems, Nanterre, France) equipped with a Photometric Cool-Snap camera (Roper Scientific, Ottobrunn, Germany). Cell culture images for counting were taken with a 20× objective in black and white for the BC binding analysis, with 10× objective for the counting of Ptc-positive cells on slices, and magnification or fluorescent images were taken with a 40× objective.

## Results

**Potency of MRT-83.** We recently described the synthesis and characterization of a novel series of molecules displaying antagonist properties toward the mouse Smo receptor. Among these molecules, the acylthiourea MRT-10 and its corresponding acylurea derivative MRT-14 were the most potent (Manetti et al., 2010). They displayed a potency comparable with that of the steroidal alkaloid cyclopamine extracted from corn lilies, which has been widely used for blocking the Hh pathway both in vitro and in vivo (Scales and de Sauvage, 2009). During our efforts to identify more potent high-affinity Smo antagonists, we have optimized the structure of MRT-10 and MRT-14 and we have now developed and synthesized MRT-83, which belongs to a new family of acylguanidine molecules (Fig. 1).

We have investigated the antagonist properties of MRT-83 toward Hh pathway activation in various cell-based assays and compared its potency with that of cyclopamine. Thus, the antagonist properties of MRT-83 and cyclopamine were determined in Shh-light2 cells, a NIH3T3 cell line stably transfected with a Gli-dependent Firefly luciferase reporter widely used for identifying Hh inhibitors (Taipale et al., 2000). These cells were stimulated for 40 h with ShhN (5 nM) in the presence or absence of the drugs in parallel experiments. We also evaluated their ability to inhibit SAG (0.1 $\mu$M)-induced differentiation of the mesenchymal pluripotent C3H10T1/2 cells into alkaline

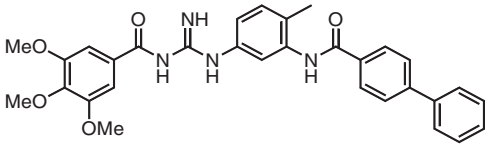


**MRT-83**

**Fig. 1.** Chemical structure of MRT-83.

phosphatase-positive osteoblasts, a response that involves activation of Smo (Hyman et al., 2009). Both molecules were found to block these responses (Fig. 2, A and B), and analysis of the dose-response curves led to an $IC_{50} \approx 10$ nM for MRT-83, which was very similar in the two assays (Table 1). These data indicate that MRT-83 is a potent Hh inhibitor that displays a greater potency (20- –60-fold) than cyclopamine.

It has been demonstrated previously that cerebellar GCPs proliferate in response to Hh activation, an effect that can be inhibited by Smo antagonists (Charytoniuk et al., 2002a; Romer et al., 2004). To further investigate the antagonist properties of MRT-83 toward this response, we analyzed its potency to inhibit rat GCP proliferation in primary culture as measured by [$^3$H]thymidine incorporation. Increasing concentrations of ShhN or SAG to rat GCPs caused a dose-dependent increase in [$^3$H]thymidine incorporation over basal level (Supplemental Fig. 1). In these experiments, the $EC_{50}$ values for ShhN and SAG were 3.2 ± 0.3 and 4.6 ± 0.2 nM, respectively. Neither MRT-83 nor cyclopamine (1 $\mu$M) modified significantly the basal level of [$^3$H]thymidine incorporation in rat GCPs (data not shown). However, MRT-83 displayed full antagonist properties with an $IC_{50}$ (~3 nM) for inhibiting ShhN (3 nM)-induced proliferation of rat GCPs (Fig. 2C and Table 1). MRT-83 also blocked SAG (0.01 $\mu$M)-induced proliferation of GCPs ($IC_{50} \approx 6$ nM) (Fig. 2C). When the same experiment was repeated in the presence of a ten fold higher SAG concentration (0.1 ìM), the dose-response curve was shifted to the right and the $IC_{50}$ for MRT-83 was increased as expected for a competitive antagonism. MRT-83 resulted in $IC_{50}$ values of 66 nM under these conditions, corresponding to an 11 fold $IC_{50}$ shift, suggesting Smo as the target of MRT-83 (Fig. 2C). MRT-83 was consistently a better antagonist than cyclopamine in these tests (Table 1).

**MRT-83 Binding to Cells Expressing Mouse and Human Smo.** To further investigate the binding properties of MRT-83 to Smo, we analyzed whether it can compete with BC, which interacts with Smo at the level of its heptahelical bundle (Chen et al., 2002b). First, we showed that BC bound to HEK293 cells stably expressing the human Smo (HEK-hSmo), as determined by fluorescence microscopy and immunostaining for the Smo protein (Supplemental Fig. 2), whereas BC did not bind to HEK293 cells not transfected with human Smo (data not shown). Then, the cells were incubated with 5 nM BC for 2 h in the presence or absence of various concentrations of MRT-83. At the end of the incubation, the cells were fixed and counterstained with DAPI. MRT-83 blocked BC binding to HEK-hSmo cells in a dose-dependent manner with an $IC_{50}$ of 4.6 nM (Fig. 2, D and E, and Table 1). We also conducted similar experiments in HEK293 cells transiently transfected for expression of mouse Smo as described previously (Manetti et al., 2010). MRT-83 abrogated BC binding to cells expressing mouse Smo with an $IC_{50}$ of 14 nM (Table 1), which was in good correlation with its $IC_{50}$ in the Shh-light2 and alkaline phosphatase assays (Table 1). All together, these data demonstrate that MRT-83 is a potent antagonist of human and mouse Smo receptors.

**MRT-83 Does Not Block Wnt Signaling.** Smo presumably belongs to the family of GPCRs and displays the highest homology with the serpentine Frizzled receptors that are responsible for Wnt signaling (van Amerongen and Nusse, 2009). To further investigate the potential activities of MRT-83 toward the Wnt pathway, we subsequently evaluated the ability of MRT-83 to modulate Wnt signaling in HEK293 transiently transfected with a Tcf/Lef-dependent Firefly luciferase reporter together with an *R. reniformis* luciferase control reporter (Fig. 3). Tcf/Lef-dependent luciferase activity was stimulated (around 40 times the basal level) in these cells when they were cotransfected with a Wnt3a plasmid compared with a control plasmid. This activity was completely blocked by the Wnt antagonist IWR1 (10

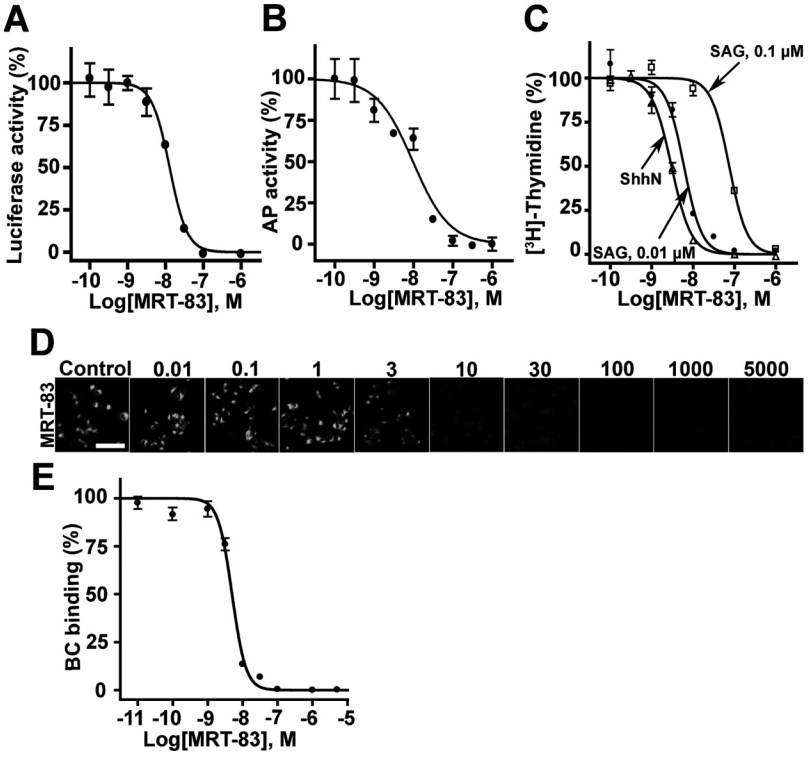


**Fig. 2.** MRT-83 inhibits Hh pathway activation in cell-based assay and BC binding to human Smo. A to C, activity of MRT-83 on ShhN-induced Gli-dependent luciferase activity in Shh-light2 cells (A), SAG-induced differentiation of C3H10T1/2 cells (B), and ShhN and SAG-induced proliferation of rat cerebellar GCPs (C). Inhibition curves were generated using increasing concentrations of MRT-83 in the presence of ShhN (5 nM; A) or (3 nM; C, △), SAG (0.1 $\mu$M) (B and C, □), or SAG (0.01 $\mu$M) (C, ●). The values are expressed as a percentage of the maximal response induced by ShhN or SAG, respectively. D, HEK-hSmo cells stably expressing human Smo were incubated with BC (5 nM) alone (Control) or in the presence of increasing concentrations (nanomolar) of MRT-83. BC binding (green) is visualized using fluorescence microscopy in a representative field (100–150 cells are shown; scale barm 50 $\mu$M). E, the concentration-response curve for MRT-83 was obtained by quantification of the BC fluorescence in three photographs for each coverslip as described under *Materials and Methods*. The values are expressed as percentage of the fluorescence detected in control HEK-hSmo cells incubated with BC alone. The data are representative of independent experiments ($n$ = 3–10) and are the means ± S.E.M. of triplicates (A and E) or quadruplicates (B and C).

TABLE 1

Compared activities of MRT-83 and cyclopamine in different cell-based assays

$IC_{50}$ values of the compounds were determined on Gli-dependent luciferase reporter activity induced by ShhN (5 nM) in Shh-light2 cells (1); AP activity induced by SAG (0.1 $\mu$M) in C3H10T1/2 cells (2); Proliferative activity of cerebellar GCPs induced by ShhN (3 nM) determined by [$^3$H]thymidine incorporation (3); BC binding to HEK293 cells stably expressing human Smo (hSmo) (4); or transiently expressing mouse Smo (mSmo) (5). Data are the means ± S.E.M. of at least three independent experiments.

| | $IC_{50}$ | | | | |
|---|---|---|---|---|---|
| | Shh-Light2 (1) | C3H10T1/2 (2) | GCPs (3) | BC Binding | |
| | | | | hSmo (4) | mSmo (5) |
| | | | *nM* | | |
| MRT-83 | 15 ± 2 | 10 ± 2 | 2.9 ± 0.5 | 4.6 ± 0.7 | 14 ± 2 |
| Cyclopamine | 300 ± 50 | 620 ± 30 | 100 ± 6 | 64 ± 17 | 50 ± 10 |

$\mu$M), as expected (Chen et al., 2009). However, MRT-83 (5 $\mu$M) did not modify significantly the basal level or the Wnt3a Tcf/Lef-dependent luciferase activity (Fig. 3).

**Smo Trafficking at the Primary Cilium Is Inhibited by MRT-83.** Smo activation was recently proposed to require a two-step mechanism including the accumulation of Smo at the primary cilium followed by an essential second activation step. These steps can be pharmacologically separated through the use of selective inhibitors and might be crucial for Smo antagonist efficacy (Rohatgi et al., 2009). To further examine the mechanism of action of MRT-83, we investigated the ability of MRT-83 to modulate the trafficking of endogenous mouse or human Smo to the primary cilium of C3H10T1/2 or of NT2 cells that derive from a pluripotent human testicular carcinoma (Fig. 4 and Supplemental Fig. 3). In basal culture conditions, Smo was not detected at the primary cilium visualized by the acetylated tubulin positive signal in both cell lines (Fig. 4A, and Supplemental Fig. 3A). After treatment with the Smo agonist SAG (1 $\mu$M) for 18 h, Smo accumulation was induced at the primary cilium as shown by the colocalization of acetylated tubulin and Smo-positive immunolabelings. This effect was blocked when the cells were incubated in the presence of MRT-83 (5 $\mu$M), whereas this compound did not promote Smo-positive signals at the primary cilium when it was administered alone. Under the same experimental conditions, cyclopamine (5 $\mu$M) was as effective as SAG (1 $\mu$M) for inducing accumulation of Smo-positive signals at the primary cilium, as evidenced in C3H10T1/2 cells (Supplemental Fig. 4, A and B), which is in agreement with its ability to promote Smo trafficking in other cells (Rohatgi et al., 2009). Thus, these data demonstrate that MRT-83 abrogates Smo ciliary translocation promoted by SAG.

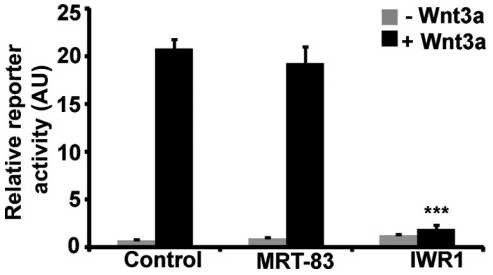


**Fig. 3.** MRT-83 does not block Wnt signaling. HEK293 cells were transiently transfected with plasmids containing Tcf/Lef-Luciferase reporter and *R. reniformis* luciferase control and, as indicated, with Wnt3a. MRT-83 (5 $\mu$M), IWR1 (10 $\mu$M), or vehicle (DMSO) alone was added into the medium 1 h after transfection, and luciferase activities were measured 48 h later. The values are expressed as arbitrary units (AU). The data are representative of independent experiments ($n = 3$) and are the means ± S.E.M. of quadruplicates. ***, $p < 0.005$.

**MRT-83 Inhibits Shh Signaling in the Subventricular Zone of the Lateral Ventricle.** The SVZ bordering the lateral ventricle (LV) constitutes one of the main neurogenic areas of the brain. Shh, Ptc and Smo have been identified within this niche (Charytoniuk et al., 2002b; Ahn and Joyner, 2005; Palma et al., 2005; Angot et al., 2008). It offers a convenient in vivo model to analyze Hh pathway regulation as previously shown by the up-regulation of Ptc transcription after the intracerebroventricular injection of ShhN (Charytoniuk et al., 2002b; Loulier et al., 2006). To test further whether MRT-83 was able to modulate this well characterized Hh-associated response in vivo, we performed stereotaxic injections of ShhN in the presence or in the absence of MRT-83 into the LV of adult mice as described under *Materials and Methods*. We investigated also the effect of MRT-36, a compound structurally related to MRT-83 but without significant activity toward Smo (Supplemental Fig. 4). As expected, a strong induction of Ptc transcription visualized by intense ISH-associated signals was observed in the SVZ of animals injected with ShhN alone compared with vehicle-treated animals (Fig. 5, B and C), which was further confirmed by quantification of $Ptc^+$ cells (vehicle, 5.1 ± 2.2; ShhN, 30 ± 4 $Ptc^+$ cells/section; total number of counted slices, $n = 10$) (Fig. 5F). Animals treated with ShhN in the presence of MRT-83 were as healthy as those of the other groups but up-regulation of Ptc transcription in the SVZ of these animals was no longer observed in agreement with a complete inhibition of ShhN-mediated effects (8.7 ± 2.4 $Ptc^+$ cells/section, $n = 9$) and was not different from vehicle-mediated effects. Conversely, the coinjection of MRT-36 did not alter ShhN-induced Ptc transcription in a significant manner (23 ± 4 $Ptc^+$ cells/section, $n = 8$; Fig. 5, D–F). Ptc expression

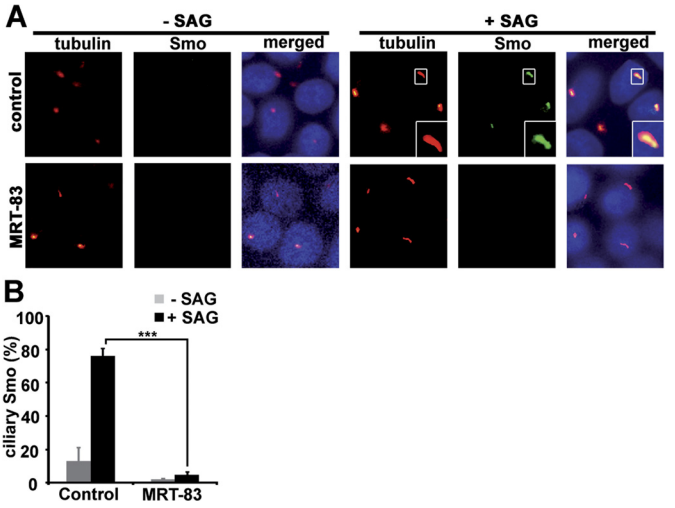


**Fig. 4.** MRT-83 abrogates Smo translocation to the primary cilium. NT2 cells untreated or treated with SAG (1 $\mu$M) alone or in the presence of MRT-83 (5 $\mu$M) were stained with antibodies against endogenous Smo (green), acetylated tubulin (red), and DAPI (blue). A, in the absence of SAG, Smo is not detected at the cilium. Cell exposure to SAG induces Smo trafficking to the cilium as identified by immunofluorescence, which is abolished by MRT-83. MRT-83 by itself does not induce Smo trafficking to the primary cilium. B, quantification of the percentage of Smo-positive cilium after treatment with the indicated compounds for 18 h. Values are the means of three to four independent experiments ± S.E.M. ***, $p < 0.005$.

profile in the MS was not altered by vehicle or ShhN injection in the SVZ or by the coinjection of Shh with MRT-36 or MRT-83 (Fig. 5, B–E, bottom panels; Fig. 5G). These data demonstrate that MRT-83 antagonizes Shh-mediated pathway activation in vivo in the SVZ.

**Pharmacophoric Model of MRT-83.** We have recently built a pharmacophoric model of Smo antagonists constituted by six features represented by three hydrogen bond acceptor groups and three hydrophobic regions (Manetti et al., 2010). MRT-83 features the following structural elements: an electron-rich phenyl ring (3,4,5-trimethoxy-substituted) linked through an acylguanidine function, to a second phenyl bearing a phenyl carbamoyl residue (Fig. 6). Superposition of MRT-83 to the model shows a perfect fit between the chemical portions of the inhibitor and the pharmacophoric features. In fact, the fit value, describing the complementarity between chemical portions of MRT-83 and the features of the model, is 5.2 of a maximum value of 6.0 (a six-feature pharmacophoric model allows, by definition, a maximum fit value of 6.0). The oxygen atom of one of the methoxy groups maps HBA1, whereas the oxygen atoms of the carbonyl moieties correspond to HBA2 and HBA3. Each of the hydrophobic regions is mapped by a phenyl ring of MRT-83. The fact that the pharmacophoric model is fully superposable to MRT-83 correlates with the high potency found for this compound.

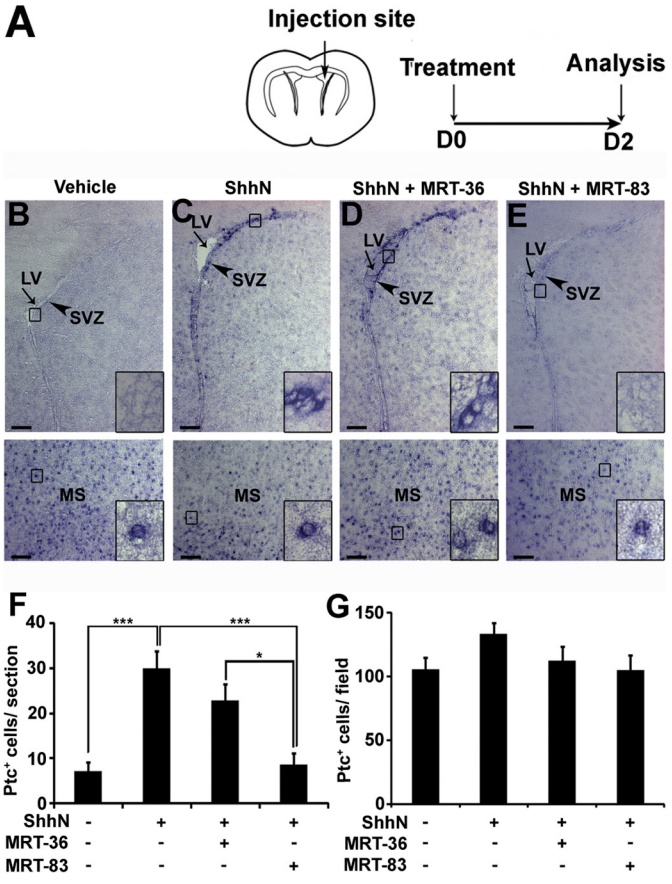


**Fig. 5.** MRT-83 antagonizes Shh signaling in vivo. A, scheme of the experimental protocol. B to E, MRT-83 but not MRT-36 antagonizes the up-regulation of Ptc transcription induced by ShhN in vivo in the SVZ of the LV. B to E, ISH experiments visualize Ptc-expressing cells (dark blue) on coronal brain sections (B–E) from control mice injected with vehicle (B) and from animals that have received ShhN (0. 9 $\mu$g) alone (C) or in the presence of MRT-36 (110 ng; D) or MRT-83 (200 ng; E). B to E, bottom, show the corresponding MS area where the pattern of Ptc expression is not modified. Quantification of the number of Ptc-expressing cells in the SVZ (F) or MS (G) for each experimental condition. Data are the means ± S.E.M. from five or six mice per group. *, $p < 0.05$; ***, $p < 0.005$. Scale bars, 200 $\mu$m.

## Discussion

In this study, we have reported the functional activity and the mechanisms of action of MRT-83, a potent acylguanidine that belongs to a novel family of Smo antagonists. The Hh pathway plays a major role in stem cell maintenance both during embryogenesis and in adult tissues, and perturbations of this pathway have been associated with human diseases, including a diverse set of cancers. The Smo receptor is an essential element in Hh signaling and Smo has been proposed as a molecular target for the action of antagonists aimed at blocking the Hh pathway in those cancers (Beachy et al., 2004; Scales and de Sauvage, 2009; Barakat et al., 2010; Peukert and Miller-Moslin, 2010).

The small-molecule inhibitor GDC-0449 holds great promise for treating metastatic BCC and medulloblastoma driven by mutations in the Hh pathway as well as several Hh-dependent cancers not linked to Hh pathway mutations (Scales and de Sauvage, 2009). However, a Smo mutation (D473H) arising within the sixth putative transmembrane domain of Smo and disrupting the ability of GDC-0449 to bind Smo was found in the tumor of a patient with medulloblastoma who had relapsed after an initial response to the drug (Rudin et al., 2009; Von Hoff et al., 2009). A Smo mutation occurring at a homologous position in mouse Smo was also observed in a GDC-0449-resistant mouse model of medulloblastoma (Yauch et al., 2009). Therefore, the development and characterization of novel Smo antagonists have valuable therapeutic interests.

Using a pharmacophoric model-based virtual screening strategy, we have recently reported the identification of the acylthiourea MRT-10 and the acylurea MRT-14 as members of novel families of Smo antagonists (Manetti et al., 2010). These new leads have rapidly allowed us to develop a new series of Smo inhibitors with high potency to which MRT-83

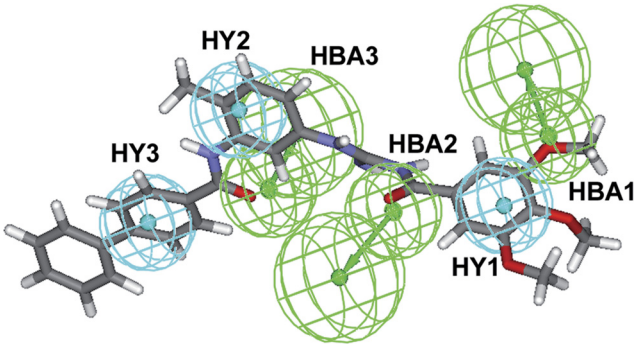


**Fig. 6.** Pharmacophoric model of MRT-83. Graphical representation of MRT-83 fitted to the proposed pharmacophoric model for Smo antagonists. Chemical features of MRT-83 are able to perfectly map all the features of the model. Features are color-coded: cyan, hydrophobic regions (HY1–3); green, hydrogen bond acceptor groups (HBA1–3). Each of the HBA features is constituted by two green spheres: the smaller is filled by the hydrogen bond acceptor atom of the inhibitor, and the larger sphere is located at the end of a vector and represents the region at which the corresponding hydrogen bond donor group of the receptor counterpart should be located. The atoms are color-coded: gray, carbon; white, hydrogen; red, oxygen; and blue, nitrogen.

belongs (this work and data not shown). MRT-83 perfectly fits with the proposed pharmacophoric model for Smo antagonists that we have recently proposed. With respect to MRT-10 or MRT-14, MRT-83 features the following structural differences: 1) a guanidine replaces the thiourea or urea functions; 2) a methyl residue is introduced in the central phenyl ring; and 3) the lateral amide is formed with biphenylcarboxylic acid. These discrete structural differences may account for the increased potency of MRT-83 observed in various in vitro Hh-based assays (Manetti et al., 2010). It is noteworthy that MRT-83 inhibits BC binding to human Smo and ShhN-mediated proliferation of GCPs with a nanomolar potency similar to that of GDC-0449 (Robarge et al., 2009). Therefore, MRT-83 seems to be one of the most potent Smo antagonists known so far. Within the family of GPCRs, cross-talk pharmacology between members displaying significant homology has been observed, such as between the calcium-sensing receptor and the related GPCRC6A receptor (Faure et al., 2009; Rosenbaum et al., 2009). Because Smo displays the highest amino acid homology with the Frizzled receptors (van Amerongen and Nusse, 2009), it was of interest to further investigate the specificity of MRT-83 toward the Wnt pathway. Our experiments demonstrate that MRT-83 did not display significant agonist or antagonist Wnt signaling activity evaluated by a Tcf/Lef dependent luciferase assay. These data indicate that MRT-83 should be a valuable tool for investigating Hh signaling mechanisms in cell culture or tissues where both pathways are functional.

The existence of multiple binding sites for both Smo agonists and antagonists might underlie for the diversity of actions of Smo positive and negative modulators. For example, the agonist SAG and the antagonist cyclopamine binding sites are overlapping but not identical (Chen et al., 2002b). Radioligand binding analysis with tritiated SAG derivatives also revealed that the antagonist SANT-1 binds in a manner consistent with that of an allosteric modulation (Rominger et al., 2009). Itraconazole, an antifungal compound, has been shown to inhibit Hh signaling and to act on Smo at a site distinct from cyclopamine (Kim et al., 2010). Whether the site of action of glucocorticoid-derived Smo agonists is overlapping with one of the above-mentioned sites is not yet known (Wang et al., 2010). Here, we have shown that MRT-83 abrogates BC binding to mouse and human Smo and suppresses the accumulation of Smo at the primary cilium induced by Hh pathway activation, whereas cyclopamine by itself induces Smo trafficking at the primary cilium in various cell lines (Supplemental Fig. 3 and Rohatgi et al., 2009; Wang et al., 2009; Wilson et al., 2009). Therefore, it might be anticipated that MRT-83 interacts with Smo. Further experiments should investigate the site of MRT-83 binding on the receptor.

It is noteworthy that primary cilia are present on human BCC and medulloblastoma and can both mediate and suppress Hh-dependent tumorigenesis (Han et al., 2009; Wong et al., 2009). Moreover, the presence of primary cilium in specific variants of human medulloblastomas is also informative from a therapeutic point of view. Thus, ciliated medulloblastomas with high Hh signaling might be susceptible to treatments that target primary cilium (Han et al., 2009). Smo activation and its regulation by Hh signaling and by small molecules at the level of the primary cilium have been proposed as a key step in tumorigenesis-dependent processes but are still not sufficiently studied (Scales and de Sauvage, 2009). It has been proposed that Smo activation requires first its translocation to the primary cilium, which is then followed by a second activation step. Thus, Smo inhibitors have been classified into at least two families of compounds. Sant1-like molecules that would block Smo trafficking to the primary cilium and cyclopamine-like molecules that would affect Smo activation process within the cilium (Rohatgi et al., 2009). The $Smo^{M2}$ mutation has been associated with BCC and a $Smo^{M2}$ protein is equally distributed in the cytoplasm and in the primary cilium of transfected cells (Rohatgi et al., 2009). It is noteworthy that the $Smo^{M2}$ protein is less sensitive to cyclopamine than WT Smo, whereas Sant1 inhibits both proteins with similar potency (Chen et al., 2002a). It has been anticipated that $Smo^{M2}$-like mutations that might arise from drug treatment in the clinic will therefore be more sensitive to the Sant1-like family of molecules than to the cylopamine-like family of molecules.

Our current work indicates that MRT-83 blocks trafficking to the primary cilium of both endogenous mouse and human Smo expressed in C3H10T1/2 cells or on human pluripotent testicular carcinoma cells. Thus, this Smo inhibitor falls into the SANT-1-like family of molecules. Further studies should clarify the molecular and biochemical mechanisms underlying the resistance to Smo inhibitors, particularly at the level of the primary cilium in normal and cancer cells.

Cyclopamine blocks Hh signaling by directly binding Smo and slows down the growth of tumors in various animal models (Beachy et al., 2004; Scales and de Sauvage, 2009). When applied in vivo, cyclopamine also inhibits stem cell proliferation in the adult SVZ (Palma et al., 2005). However, it was recently proposed that cyclopamine and another unrelated Smo antagonist may have nonspecific off-target effects on cell growth (Yauch et al., 2008). Thus, it was of interest to further investigate the ability of MRT-83 to modulate Hh signaling in vivo. We have previously observed that direct infusion of Shh into the LV of rodent brain induced a rapid Ptc transcription in the SVZ, indicating that Hh pathway is activated in this neurogenic area (Loulier et al., 2006). In the present study, such Ptc transcription was also observed 2 days after Shh infusion in the LV, as identified by the strong ISH signals detected in the cells located throughout the SVZ of treated animals, whereas such signals were not present in control animals. These signals were not observed in the SVZ areas of brain sections from animals treated with MRT-83 but were present when animals were treated with MRT-36, a molecule sharing structural homology with MRT-83 but not harboring Hh pathway inhibitory or stimulatory properties (Supplemental Fig. 4). ShhN injection was not accompanied by up-regulation of Ptc transcription in the adjacent septum in agreement with previous work (Charytoniuk et al., 2002b) and Ptc expression profile in this area was not modified either by the coadministration of MRT-83 or MRT-36 with ShhN. All together, these data demonstrate that MRT-83 is a potent antagonist of ShhN-induced up-regulation of Ptc transcription in the SVZ. Both Smo and Ptc are expressed in cells located in the SVZ (Angot et al., 2008). Thus, because MRT-83 is a potent Smo inhibitor in various in vitro-based assays, Hh pathway inhibition in the SVZ may reflect Smo blockade in this neurogenic area.

Blocking the Hh pathway seems to be a promising approach for the treatment of various types of cancers. There-

fore, understanding the mode of action of Smo inhibitors as well as delineating their pharmacological and functional properties is an important goal for further development of a new class of therapeutic molecules in oncology. Thus, MRT-83, which is a novel potent Smo antagonist belonging to a acylguanidine family of molecules, should be a valuable tool for further investigating the mode of action of Smo inhibitors and for characterizing Smo functions both in vitro and in vivo.

**Acknowledgments**

We thank Dr. R. Moon (University of Washington, Seattle, WA) for kindly providing the Super8xTOPFlash reporter plasmid and Dr. J. Kitajewski (Columbia University, New York, NY) for the pLNC Wnt-3aHA plasmid. We thank Dr. S. O'Regan for critical reading of the manuscript.

**Authorship Contributions**

*Participated in research design:* Roudaut, Traiffort, Faure, Ruat, Solinas, and Taddei.

*Conducted experiments:* Roudaut, Traiffort, Gorojankina, and Faure.

*Contributed new reagents or analytic tools:* Vincent, Schoenfelder, Mann, Solinas, Taddei, and Manetti.

*Performed data analysis:* Roudaut, Traiffort, Gorojankina, Faure, and Ruat.

*Wrote or contributed to the writing of the manuscript:* Roudaut, Ruat, and Manetti.

**References**

Ahn S and Joyner AL (2005) In vivo analysis of quiescent adult neural stem cells responding to Sonic hedgehog. *Nature* **437:**894–897.

Angot E, Loulier K, Nguyen-Ba-Charvet KT, Gadeau AP, Ruat M, and Traiffort E (2008) Chemoattractive activity of sonic hedgehog in the adult subventricular zone modulates the number of neural precursors reaching the olfactory bulb. *Stem Cells* **26:**2311–2320.

Barakat MT, Humke EW, and Scott MP (2010) Learning from Jekyll to control Hyde: Hedgehog signaling in development and cancer. *Trends Mol Med* **16:**337–348.

Beachy PA, Karhadkar SS, and Berman DM (2004) Tissue repair and stem cell renewal in carcinogenesis. *Nature* **432:**324–331.

Charytoniuk D, Porcel B, Rodríguez Gomez J, Faure H, Ruat M, and Traiffort E (2002a) Sonic Hedgehog signalling in the developing and adult brain. *J Physiol Paris* **96:**9–16.

Charytoniuk D, Traiffort E, Hantraye P, Hermel JM, Galdes A, and Ruat M (2002b) Intrastriatal sonic hedgehog injection increases Patched transcript levels in the adult rat subventricular zone. *Eur J Neurosci* **16:**2351–2357.

Chen B, Dodge ME, Tang W, Lu J, Ma Z, Fan CW, Wei S, Hao W, Kilgore J, Williams NS, et al. (2009) Small molecule-mediated disruption of Wnt-dependent signaling in tissue regeneration and cancer. *Nat Chem Biol* **5:**100–107.

Chen JK, Taipale J, Cooper MK, and Beachy PA (2002a) Inhibition of Hedgehog signaling by direct binding of cyclopamine to Smoothened. *Genes Dev* **16:**2743–2748.

Chen JK, Taipale J, Young KE, Maiti T, and Beachy PA (2002b) Small molecule modulation of Smoothened activity. *Proc Natl Acad Sci USA* **99:**14071–14076.

Corbit KC, Aanstad P, Singla V, Norman AR, Stainier DY, and Reiter JF (2005) Vertebrate Smoothened functions at the primary cilium. *Nature* **437:**1018–1021.

Dessaud E, McMahon AP, and Briscoe J (2008) Pattern formation in the vertebrate neural tube: a sonic hedgehog morphogen-regulated transcriptional network. *Development* **135:**2489–2503.

Faure H, Gorojankina T, Rice N, Dauban P, Dodd RH, Bräuner-Osborne H, Rognan D, and Ruat M (2009) Molecular determinants of non-competitive antagonist binding to the mouse GPRC6A receptor. *Cell calcium* **46:**323–332.

Han YG, Kim HJ, Dlugosz AA, Ellison DW, Gilbertson RJ, and Alvarez-Buylla A (2009) Dual and opposing roles of primary cilia in medulloblastoma development. *Nat Med* **15:**1062–1065.

Hyman JM, Firestone AJ, Heine VM, Zhao Y, Ocasio CA, Han K, Sun M, Rack PG, Sinha S, Wu JJ, et al. (2009) Small-molecule inhibitors reveal multiple strategies for Hedgehog pathway blockade. *Proc Natl Acad Sci USA* **106:**14132–14137.

Kim J, Tang JY, Gong R, Kim J, Lee JJ, Clemons KV, Chong CR, Chang KS, Fereshteh M, Gardner D, et al. (2010) Itraconazole, a commonly used antifungal that inhibits Hedgehog pathway activity and cancer growth. *Cancer Cell* **17:**388–399.

Li JJ, Shanmugasundaram V, Reddy S, Fleischer LL, Wang Z, Smith Y, Harter WG, Yue WS, Swaroop M, Li L, et al. (2010) Smoothened antagonists for hair inhibition. *Bioorg Med Chem Lett* **20:**4932–4935.

Lin AC, Seeto BL, Bartoszko JM, Khoury MA, Whetstone H, Ho L, Hsu C, Ali SA, Ali AS, and Alman BA (2009) Modulating hedgehog signaling can attenuate the severity of osteoarthritis. *Nat Med* **15:**1421–1425.

Loulier K, Ruat M, and Traiffort E (2006) Increase of proliferating oligodendroglial progenitors in the adult mouse brain upon Sonic hedgehog delivery in the lateral ventricle. *J Neurochem* **98:**530–542.

Manetti F, Faure H, Roudaut H, Gorojankina T, Traiffort E, Schoenfelder A, Mann A, Solinas A, Taddei M, and Ruat M (2010) Virtual screening-based discovery and mechanistic characterization of the acylthiourea MRT-10 family as smoothened antagonists. *Mol Pharmacol* **78:**658–665.

Martínez MC, Larbret F, Zobairi F, Coulombe J, Debili N, Vainchenker W, Ruat M, and Freyssinet JM (2006) Transfer of differentiation signal by membrane microvesicles harboring hedgehog morphogens. *Blood* **108:**3012–3020.

Masdeu C, Bernard V, Faure H, Traiffort E, and Ruat M (2007) Distribution of Smoothened at hippocampal mossy fiber synapses. *Neuroreport* **18:**395–399.

Palma V, Lim DA, Dahmane N, Sánchez P, Brionne TC, Herzberg CD, Gitton Y, Carleton A, Alvarez-Buylla A, and Ruiz i Altaba A (2005) Sonic hedgehog controls stem cell behavior in the postnatal and adult brain. *Development* **132:**335–344.

Peukert S and Miller-Moslin K (2010) Small-molecule inhibitors of the hedgehog signaling pathway as cancer therapeutics. *Chem Med Chem* **5:**500–512.

Robarge KD, Brunton SA, Castanedo GM, Cui Y, Dina MS, Goldsmith R, Gould SE, Guichert O, Gunzner JL, Halladay J, Jia W, Khojasteh C, Koehler MF, Kotkow K, La H, Lalonde RL, Lau K, Lee L, Marshall D, Marsters JC, Jr., Murray LJ, Qian C, Rubin LL, Salphati L, Stanley MS, Stibbard JH, Sutherlin DP, Ubhayaker S, Wang S, Wong S, and Xie M (2009) GDC-0449-a potent inhibitor of the hedgehog pathway. *Bioorg Med Chem Lett* **19:**5576–5581.

Rohatgi R, Milenkovic L, Corcoran RB, and Scott MP (2009) Hedgehog signal transduction by Smoothened: pharmacologic evidence for a 2-step activation process. *Proc Natl Acad Sci USA* **106:**3196–3201.

Rohatgi R, Milenkovic L, and Scott MP (2007) Patched1 regulates hedgehog signaling at the primary cilium. *Science* **317:**372–376.

Romer JT, Kimura H, Magdaleno S, Sasai K, Fuller C, Baines H, Connelly M, Stewart CF, Gould S, Rubin LL, et al. (2004) Suppression of the Shh pathway using a small molecule inhibitor eliminates medulloblastoma in Ptc1(+/−)p53(−/−) mice. *Cancer cell* **6:**229–240.

Rominger CM, Bee WL, Copeland RA, Davenport EA, Gilmartin A, Gontarek R, Hornberger KR, Kallal LA, Lai Z, Lawrie K, et al. (2009) Evidence for allosteric interactions of antagonist binding to the smoothened receptor. *J Pharmacol Exp Ther* **329:**995–1005.

Rosenbaum DM, Rasmussen SG, and Kobilka BK (2009) The structure and function of G-protein-coupled receptors. *Nature* **459:**356–363.

Rudin CM, Hann CL, Laterra J, Yauch RL, Callahan CA, Fu L, Holcomb T, Stinson J, Gould SE, Coleman B, et al. (2009) Treatment of medulloblastoma with hedgehog pathway inhibitor GDC-0449. *N Engl J Med* **361:**1173–1178.

Scales SJ and de Sauvage FJ (2009) Mechanisms of Hedgehog pathway activation in cancer and implications for therapy. *Trends Pharmacol Sci* **30:**303–312.

Taipale J, Chen JK, Cooper MK, Wang B, Mann RK, Milenkovic L, Scott MP, and Beachy PA (2000) Effects of oncogenic mutations in Smoothened and Patched can be reversed by cyclopamine. *Nature* **406:**1005–1009.

Traiffort E, Angot E, and Ruat M (2010) Sonic Hedgehog signaling in the mammalian brain. *J Neurochem* **113:**576–590.

van Amerongen R and Nusse R (2009) Towards an integrated view of Wnt signaling in development. *Development* **136:**3205–3214.

Von Hoff DD, LoRusso PM, Rudin CM, Reddy JC, Yauch RL, Tibes R, Weiss GJ, Borad MJ, Hann CL, Brahmer JR, Mackey HM, Lum BL, Darbonne WC, Marsters JC, Jr., de Sauvage FJ, and Low JA (2009) Inhibition of the hedgehog pathway in advanced basal-cell carcinoma. *N Engl J Med* **361:**1164–1172.

Wang J, Lu J, Bond MC, Chen M, Ren XR, Lyerly HK, Barak LS, and Chen W (2010) Identification of select glucocorticoids as Smoothened agonists: potential utility for regenerative medicine. *Proc Natl Acad Sci USA* **107:**9323–9328.

Wang Y, Zhou Z, Walsh CT, and McMahon AP (2009) Selective translocation of intracellular Smoothened to the primary cilium in response to Hedgehog pathway modulation. *Proc Natl Acad Sci USA* **106:**2623–2628.

Wilson CW, Chen MH, and Chuang PT (2009) Smoothened adopts multiple active and inactive conformations capable of trafficking to the primary cilium. *PLoS One* **4:**e5182.

Wong SY, Seol AD, So PL, Ermilov AN, Bichakjian CK, Epstein EH, Jr., Dlugosz AA, and Reiter JF (2009) Primary cilia can both mediate and suppress Hedgehog pathway-dependent tumorigenesis. *Nat Med* **15:**1055–1061.

Yam PT, Langlois SD, Morin S, and Charron F (2009) Sonic hedgehog guides axons through a noncanonical, Src-family-kinase-dependent signaling pathway. *Neuron* **62:**349–362.

Yauch RL, Dijkgraaf GJ, Alicke B, Januario T, Ahn CP, Holcomb T, Pujara K, Stinson J, Callahan CA, Tang T, et al. (2009) Smoothened mutation confers resistance to a Hedgehog pathway inhibitor in medulloblastoma. *Science* **326:**572–574.

Yauch RL, Gould SE, Scales SJ, Tang T, Tian H, Ahn CP, Marshall D, Fu L, Januario T, Kallop D, et al. (2008) A paracrine requirement for hedgehog signalling in cancer. *Nature* **455:**406–410.

**Address correspondence to:** Martial Ruat, CNRS, UPR-3294, Laboratoire de Neurobiologie et Développement, Institut de Neurobiologie Alfred Fessard IFR2118, Signal Transduction and Developmental Neuropharmacology team, 1 avenue de la Terrasse, F-91198, Gif-sur-Yvette, France. E-mail: ruat@inaf.cnrs-gif.fr